

Isogeometric method based in-plane and out-of-plane free vibration analysis for Timoshenko curved beams

Hongliang Liu¹, Xuefeng Zhu² and Dixiong Yang^{*1}

¹Department of Engineering Mechanics, State Key Laboratory of Structural Analysis for Industrial Equipment, Dalian University of Technology, Dalian 116023, China

²School of Automobile Engineering, Dalian University of Technology, Dalian 116023, China

(Received July 15, 2015, Revised March 22, 2016, Accepted May 5, 2016)

Abstract. In-plane and out-of-plane free vibration analysis of Timoshenko curved beams is addressed based on the isogeometric method, and an effective scheme to avoid numerical locking in both of the two patterns is proposed in this paper. The isogeometric computational model takes into account the effects of shear deformation, rotary inertia and axis extensibility of curved beams, and is applicable for uniform circular beams, and more complicated variable curvature and cross-section beams as illustrated by numerical examples. Meanwhile, it is shown that, the C^{p-1} -continuous NURBS elements remarkably have higher accuracy than the finite elements with the same number of degrees of freedom. Nevertheless, for in-plane or out-of-plane vibration analysis of Timoshenko curved beams, the NURBS-based isogeometric method also exhibits locking effect to some extent. To eliminate numerical locking, the selective reduced one-point integration and \bar{B} projection element based on stiffness ratio is devised to achieve locking free analysis for in-plane and out-of-plane models, respectively. The suggested integral schemes for moderately slender models obtain accurate results in both dominated and non-dominated regions of locking effect. Moreover, this strategy is effective for beam structures with different slenderness. Finally, the influence factors of structural parameters of curved beams on their natural frequency are scrutinized.

Keywords: Timoshenko curved beams; in-plane and out-of-plane free vibration; isogeometric analysis; NURBS elements; numerical locking

1. Introduction

Curved beam structures have been widely utilized in bridge, building structures and industrial products. Thus, it is of importance to predict precisely the natural frequencies and modal shapes in structural design. Both in-plane and out-of-plane patterns may occur in free vibration of curved beams. As a consequence of the curvature effect, the vibration modes of curved beam are mutually coupled containing flexure, extension, shear and twisting behavior. However, in-plane and out-of-plane vibrations are decoupled when the plane containing the centerline of the undeformed beam axis is a principal plane of the cross section at every point along the bar and also a plane of material symmetry. In this case, the in-plane beam model mainly relates to the bending-extensional

*Corresponding author, Professor, E-mail: yangdx@dlut.edu.cn

modes, while the out-of-plane model involves the bending-twisting modes (Chidamparam and Leissa 1993). Therefore, the dynamic analysis of a curved beam is inconvenient owing to its complex geometry and different vibration modes.

In fact, many researchers have devoted to modeling, computational methods and numerical analysis of the relevant mechanical problems about the vibration of curved beam structures (Auciello and Rosa 1994). Various computational models and techniques are applied to solve these problems, such as finite difference method (Ball 1967), transition matrix method (Bickford and Strom 1975), finite element method (Raveendranath *et al.* 2001, Wu and Chiang 2003, Kim *et al.* 2009), wave propagation method (Kang *et al.* 2003), differential quadrature method (Kang *et al.* 1995) and dynamic stiffness method (Howson and Jemah 1999, Huang *et al.* 2000) etc. Recently, a condensation method is described for the free vibration analysis of curved beams (Mochida and Ilanko 2016). In practice, the finite element method (FEM) as a versatile numerical technique is widely used for solving complex engineering problems. Timoshenko beam theory can make a good prediction for the mechanical behavior generated by thick beam especially for the higher order vibration modes, which takes into account shear deformation and rotatory inertia (Chidamparam and Leissa 1993). However, there may be numerical locking in displacement-based finite element analysis, namely the classical elements show field inconsistency and stiffening effect, which is a common problem in full integration for the low-order elements. In general, in-plane motion involves shear and membrane locking, while it has been found that there are obvious locking effects in the context of out-of-plane motion as well (Ishaquddin *et al.* 2012, 2013).

Isogeometric analysis (IGA) is a new type of computational method proposed by Hughes *et al.* (2005), in which the NURBS and T-splines etc. of computer-aided design (CAD) representing exact geometric model are adopted as the basis functions for structural analysis. Hence, geometric design of CAD and numerical computation of computer-aided engineering (CAE) can be closely integrated to realize the structural analysis directly on exact geometry. In contrast to the traditional FEM, it is convenient to implement the model transformation of complex geometries for IGA, without introducing the geometric error. As a result, IGA has attracted so much attention that it is becoming an active area in the field of computational mechanics, owing to the superior characteristics of NURBS such as high-order continuity and geometrical invariability during the refinement (Cottrell *et al.* 2009, Kim *et al.* 2009). Among them, Cottrell *et al.* (2006) initially applied IGA for structural vibration analysis. Weeger *et al.* (2013) studied the vibration of non-linear Euler-Bernoulli straight beam. Specific to the in-plane free vibration, the Timoshenko straight and free-form curved beams were investigated by means of isogeometric approach in (Lee and Park 2013, Luu *et al.* 2015). Wang *et al.* (2013, 2015) proposed a set of higher order mass matrices to upgrade the frequency accuracy, and superconvergent free vibration analysis can be achieved for Euler-Bernoulli beams and Kirchhoff plates. Additionally, to overcome numerical locking of NURBS beam element, Echter and Bischoff (2010) introduced the discrete shear gap (DSG) method into IGA for statics analysis of straight beam, and the resulting elements are free from shear locking. However, Bouclier *et al.* (2012) further showed that the NURBS DSG elements were not efficient enough for curved beam, and the NURBS \bar{B} projection method was recommended to realize locking free analysis. It is well known that the selective reduced integration techniques are widely used in alleviating locking effect due to the simplicity of operation and low computational cost. Consequently, the improved numerical integration was discussed in detail for locking treatment in isogeometric elements (Adam *et al.* 2014).

In terms of above mentioned review, the previous researches about vibration analysis of beam structure mainly concentrated on improving the beam models and also developing new general

algorithms. For curved beams, and especially variable curvature ones, it is necessary to establish a set of new superior computational procedure appropriate for both in-plane and out-of-plane curved beam models. Furthermore, the so called k -refinement for IGA can achieve the element continuity of C^{p-1} . It requires only less degrees of freedom, and can obtain better numerical precision if the locking effect of curved beam is not dominated (Adam *et al.* 2014). Nevertheless, the above statement for IGA is obtained according to statics or in-plane vibration analysis of curved beam recently, and there is no relevant work reported for out-of-plane vibration analysis and locking elimination in both in-plane and out-of-plane free vibration. In particular, it is important to devise an effective approach for locking free analysis of Timoshenko curved beams with different slenderness and complicated cross section, and acquire the desired results in both dominated and non-dominated regions of locking.

In this paper, the in-plane and out-of-plane free vibrations of circular and parabolic Timoshenko curved beams are addressed by use of IGA with the interior element continuity of C^{p-1} . In order to overcome numerical locking, an effective scheme containing both in-plane and out-of-plane pattern is proposed to realize accurate vibration analysis of curved beams. The remained of this paper is organized as follows. In Section 2, a brief overview of NURBS-based isogeometric analysis is presented for the sake of completeness and comprehension, and the in-plane and out-of-plane free vibration formulas of curved beams are established. In Section 3, in-plane and out-of-plane locking in the context of free vibration of Timoshenko curved beam is illustrated, and a feasible integral scheme in both dominated and non-dominated regions of locking effect is devised. In Section 4, several numerical examples for in-plane and out-of-plane free vibration of circular and parabolic beams are demonstrated. The conclusions are drawn in Section 5.

2. Isogeometric free vibration formulation of Timoshenko curved beams

2.1 NURBS-based isogeometric analysis

B-splines are piecewise polynomial functions composed of the basis functions defined in the parameter space. The B-spline basis functions are constructed from a knot vector, which is the non-decreasing sequence defined as

$$\Xi = \{\xi_1, \xi_2, \dots, \xi_{n+p+1}\} \tag{1}$$

where n is the number of basis functions and p is the polynomial order. The interval $[\xi_1, \xi_{n+p+1}]$ is called a patch and the interval $[\xi_i, \xi_{i+1})$ defines a knot span. A knot vector is said to be uniform if they are equally spaced, otherwise non-uniform. And it is referred to as open if the first and last knots have multiplicity $p+1$. Open knot vectors are employed in this work to define the B-spline geometries interpolating at the first and last control points.

$N_{i,p}(\xi)$ represents the i th B-spline basis function of order p , and this definition is given according to the Cox–de Boor recursion formula (Cottrell *et al.* 2009)

$$N_{i,0}(\xi) = \begin{cases} 1, & \text{if } \xi_i \leq \xi \leq \xi_{i+1} \\ 0, & \text{otherwise} \end{cases} \tag{2}$$

$$N_{i,p}(\xi) = \frac{\xi - \xi_i}{\xi_{i+p} - \xi_i} N_{i,p-1}(\xi) + \frac{\xi_{i+p+1} - \xi}{\xi_{i+p+1} - \xi_{i+1}} N_{i+1,p-1}(\xi) \quad (3)$$

where i is the knot index and $i = 1, 2, \dots, n+p+1$.

A B-spline curve is constructed by taking a linear combination of B-spline basis functions. Given n basis $N_{i,p}$ and corresponding control points $\mathbf{P}_i \in R^d$, $i=1, 2, \dots, n$, a B-spline curve is defined as

$$C(\xi) = \sum_{i=1}^n N_{i,p}(\xi) \mathbf{P}_i \quad (4)$$

Then, a non-uniform rational B-splines (NURBS) curve in R^d is obtained by the projective transformation of a B-spline curve in R^{d+1} , which can exactly describe conic sections, such as circles and ellipses etc. The definitions of a NURBS curve and its basis function are expressed as

$$C(\xi) = \sum_{i=1}^n R_{i,p}(\xi) \mathbf{P}_i \quad (5)$$

$$R_{i,p} = \frac{w_i N_{i,p}(\xi)}{\sum_{j=1}^n w_j N_{j,p}(\xi)} \quad (6)$$

where $\mathbf{P}_i \in R^d$ represent NURBS control points, $R_{i,p}$ are the rational B-spline basis functions, and w_i indicates the i th weight.

Further, the important properties of NURBS basis functions are shown as follows (Piegl and Tiller 1997):

- 1) Non-negativity: $R_{i,p}(\xi) \geq 0$;
- 2) Partition of unity: $\sum_{i=1}^n R_{i,p}(\xi) = 1$;
- 3) $R_{1,p}(0) = R_{n,p}(1) = 1$;
- 4) Local support: If $\xi \notin [\xi_i, \xi_{i+p+1}]$, then $R_{i,p}(\xi) = 0$;
- 5) Smoothness: $R_{i,p}(\xi)$ is $p-1$ times continuously differentiable at a knot at most.

Moreover, the refinement strategies of NURBS curves (Hughes *et al.* 2005) include:

- 1) h -refinement: Knots may be inserted without changing the curve geometrically or parametrically;
- 2) p -refinement: The order of basis functions may be increased and the continuities of elements remain unchanged;
- 3) k -refinement: Order elevation followed by knot insertion, which can achieve the continuity of C^{p-1} .

In the process of structural analysis, NURBS basis functions will serve as the element shape functions based on isoparametric concept, and thus the major advantages of isogeometric approach comparing with classical Lagrange finite element analysis involve the following several aspects (Cottrell *et al.* 2009):

- 1) The exact NURBS geometry is employed for analysis instead of approximate finite element meshes.
- 2) To implement the element refinement is so simple that there is no much effort in further

communication with the CAD system, and the geometric model always keeps constant. A local model refinement in IGA can be achieved based on the work of Wang and Zhang (2014).

3) High-order continuity of NURBS overcomes the drawbacks of traditional finite element analysis, which only have C^0 -continuity between the elements in general.

4) There are fairly less number of control points in isogeometric analysis than that of finite element analysis for the same integral element number, and thus the higher computational accuracy can be obtained for IGA under the same number of degrees of freedom.

2.2 In-plane isogeometric model

The planar curved beam is considered as shown in Fig. 1, and (η, ζ) and (x, z) are defined as global and local coordinates, respectively. The x axis is located along the tangential direction of centroidal axis, and the radius of curvature R may change with x . Herein, the in-plane and out-of-plane motions are decoupled because the curved beam with symmetric cross-section is considered, and the involved variables contains the tangential displacement u , normal displacement w , and rotation θ of the cross section about the out-of-plane axis. The strain-displacement and constitutive relations of Timoshenko curved beam (Chidamparam and Leissa 1993, Raveendranath *et al.* 2001) are formulated as follows

$$\varepsilon = \frac{\partial u}{\partial x} + \frac{w}{R}, \quad \gamma = \theta + \frac{\partial w}{\partial x} - \frac{u}{R}, \quad \kappa = \frac{\partial \theta}{\partial x} \tag{7}$$

$$N = EA\varepsilon, \quad Q = kGA\gamma, \quad M = EI\kappa \tag{8}$$

where ε , γ and κ represent the membrane, transverse shear and curvature strain, respectively; N , Q and M are the axial force, shear force and bending moment, separately; A , I , E , G and k denote the area of cross section, moment of inertia, Young's modulus, shear modulus and shear correction factor, respectively. Specifically, A and I are constant for uniform curved beams, while they vary with the curvilinear coordinate x for variable cross-section beams.

For a thick curved beam, the dynamic equilibrium equation of free vibration based on the principle of virtual work is written as

$$\int_0^L (EA\varepsilon\delta\varepsilon + EI\kappa\delta\kappa + kGA\gamma\delta\gamma) dx = \int_0^L \delta u \rho A \ddot{u} dx + \int_0^L \delta w \rho A \ddot{w} dx + \int_0^L \delta \theta \rho I \ddot{\theta} dx \tag{9}$$

where L is the beam length, ρ is the mass density, δu , δw , $\delta \theta$ and $\delta \varepsilon$, $\delta \gamma$, $\delta \kappa$ are the virtual terms related to the displacement and strain, \ddot{u} , \ddot{w} and $\ddot{\theta}$ are the associated acceleration, respectively.

In this paper, the analysis of symmetric curved beam is simplified to one-dimensional

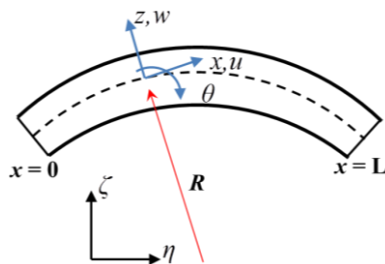


Fig. 1 In-plane curved beam model

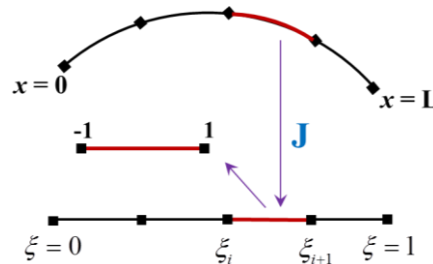


Fig. 2 NURBS computation space of curved beam elements

problems, and a NURBS curve is employed to describe exactly the centroidal axis of beam model in terms of Eq. (5). The NURBS computation space of curved beam contains the physical domain $(0, L)$ and parametric domain $(0, 1)$ as shown in Fig. 2, and their relationships can be established as follows through the Jacobian matrix \mathbf{J}

$$\begin{aligned} x &= x(\zeta) = \int_{\zeta^0=0}^{\zeta^0=\zeta} \sqrt{(\eta_{,\zeta^0})^2 + (\zeta_{,\zeta^0})^2} d\zeta^0 \\ \mathbf{J} &= x_{,\zeta} = \sqrt{(\eta_{,\zeta})^2 + (\zeta_{,\zeta})^2} \\ \frac{1}{R} &= \frac{\eta_{,\zeta} \zeta_{,\zeta\zeta} - \zeta_{,\zeta} \eta_{,\zeta\zeta}}{\mathbf{J}^3} \end{aligned} \quad (10)$$

Based on the fundamental idea of isogeometric approach, the displacement variables are discretized using NURBS basis functions, and the displacement components corresponding to control points are written as

$$\mathbf{u}(\zeta) = \sum_{i=1}^n R_i(\zeta) \mathbf{u}_i \quad (11)$$

where n is the number of control points, $\mathbf{u}=(u,w,\theta)$ and $\mathbf{u}_i=(u_i,w_i,\theta_i)$, hence the following formulas are obtained

$$\ddot{\mathbf{u}}(\zeta) = \sum_{i=1}^n R_i(\zeta) \ddot{\mathbf{u}}_i, \quad \delta \mathbf{u}(\zeta) = \sum_{i=1}^n R_i(\zeta) \delta \mathbf{u}_i \quad (12)$$

Substituting Eqs. (7), (10), (11) and (12) into Eq. (9) yields

$$\delta \mathbf{u}^T [\mathbf{K} \mathbf{u} - \mathbf{M} \ddot{\mathbf{u}}] = 0 \quad (13)$$

Due to the arbitrariness of the virtual displacement $\delta \mathbf{u}$, therefore Eq. (14) is achieved

$$\mathbf{K} \mathbf{u} - \mathbf{M} \ddot{\mathbf{u}} = 0 \quad (14)$$

where \mathbf{K} and \mathbf{M} are global stiffness matrix and mass matrix of curved beam, respectively.

Let

$$\mathbf{u} = \phi_k e^{i\omega_k t} \quad (15)$$

Substituting Eq. (15) into Eq. (14) yields the eigenvalue equation

$$[\mathbf{K} - \omega_k^2 \mathbf{M}] \phi_k = 0 \quad (16)$$

where ϕ_k is the model vector, ω_k is the corresponding natural frequency, and k denotes the k th mode. Then the subsequent solving process is similar to that of the traditional finite element analysis. The global stiffness and mass matrices of curved beam can be expressed as

$$\begin{aligned} \mathbf{K} &= \mathbf{K}_{ij} \\ &= \int_0^L \begin{bmatrix} \nabla_x R_{i,p} & -R_{i,p}/R & 0 \\ R_{i,p}/R & \nabla_x R_{i,p} & -R_{i,p} \\ 0 & 0 & \nabla_x R_{i,p} \end{bmatrix}^T \begin{bmatrix} EA & 0 & 0 \\ 0 & kGA & 0 \\ 0 & 0 & EI \end{bmatrix} \begin{bmatrix} \nabla_x R_{j,p} & -R_{j,p}/R & 0 \\ R_{j,p}/R & \nabla_x R_{j,p} & -R_{j,p} \\ 0 & 0 & \nabla_x R_{j,p} \end{bmatrix} dx \\ \mathbf{M} &= \mathbf{M}_{ij} = \int_0^L \begin{bmatrix} \rho A R_i R_j & 0 & 0 \\ 0 & \rho A R_i R_j & 0 \\ 0 & 0 & \rho I R_i R_j \end{bmatrix} dx \end{aligned} \quad (17)$$

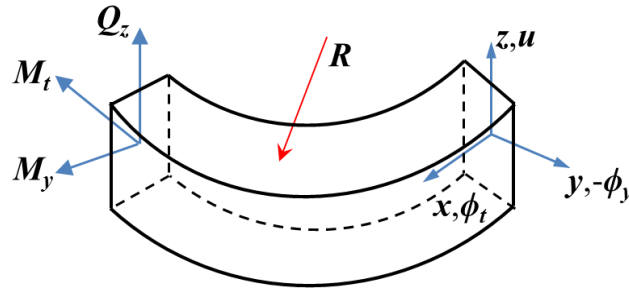


Fig. 3 Out-of-plane curved beam model

where $\nabla_x = \partial/\partial x$ is the differential operator, i, j denote the serial number of control points, and R is the radius of curvature. The non-zero knot spans can determine computational elements for isogeometric analysis, and Gaussian quadrature is adopted to integrate the stiffness and mass matrix in the interval $[-1, 1]$. Furthermore, the mechanical behavior of Timoshenko straight beam can be analyzed directly through eliminating the curvature term R , namely $1/R=0$.

2.3 Out-of-plane isogeometric model

The out-of-plane curved beam model is shown in Fig. 3, in which the coordinate system (x, y, z) is established with x axis along the tangential direction of centroidal axis, y along the normal direction, and z perpendicular to the plane (x, y) . Moreover, the cross-section variables contain the out-of-plane transverse displacement u , the bending rotation ϕ_y about y axis, and the twisting angle ϕ_t about x axis, respectively; Q_z, M_y and M_t are the associated shear force, bending moment and twisting moment. Apart from the representation of variables similar to the in-plane model, I_y, I_p and J denote the moment of inertia with respect to y axis, the polar moment of inertia and twisting constant, separately.

The corresponding elastic equations of Timoshenko curved beam with considering the effects of shear deformation and rotary inertia (Chidamparam and Leissa 1993, Huang *et al.* 2000) can be given by

$$Q_z = kGA\left(\frac{\partial u}{\partial x} - \phi_y\right), M_y = -EI_y\left(\frac{\partial \phi_y}{\partial x} + \frac{\phi_t}{R}\right), M_t = GJ\left(\frac{\partial \phi_t}{\partial x} - \frac{\phi_y}{R}\right) \tag{18}$$

Similarly, the dynamic equilibrium equation of Timoshenko curved beam for out-of-plane free vibration can be written as

$$\int_0^L [Q_z \delta\left(\frac{\partial u}{\partial x} - \phi_y\right) - M_y \delta\left(\frac{\partial \phi_y}{\partial x} + \frac{\phi_t}{R}\right) + M_t \delta\left(\frac{\partial \phi_t}{\partial x} - \frac{\phi_y}{R}\right)] dx = \int_0^L \rho A \ddot{u} \delta u \, dx + \int_0^L \rho I_y \ddot{\phi}_y \delta \phi_y \, dx + \int_0^L \rho I_p \ddot{\phi}_t \delta \phi_t \, dx \tag{19}$$

where $\delta u, \delta \phi_y$ and $\delta \phi_t$ are the associated three virtual displacements, separately. The solving procedure of Eq. (19) is identical to that of in-plane isogeometric model.

Further, the global stiffness and mass matrices of out-of-plane curved beam can be expressed as

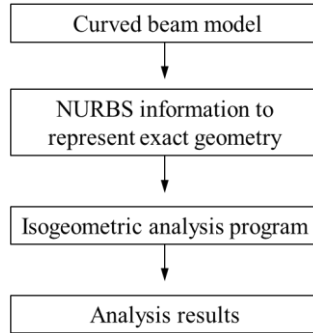


Fig. 4 IGA flow chart of Timoshenko curved beam

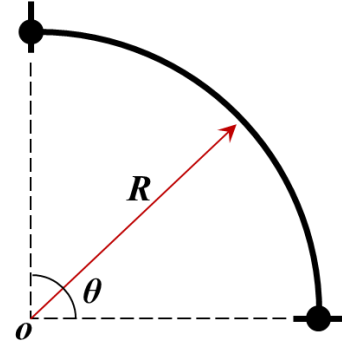


Fig. 5 A quarter of circular arch model

$$\mathbf{K} = \begin{bmatrix} K_{uu} & K_{u\phi_y} & K_{u\phi_t} \\ K_{u\phi_y}^T & K_{\phi_y\phi_y} & K_{\phi_y\phi_t} \\ K_{u\phi_t}^T & K_{\phi_y\phi_t}^T & K_{\phi_t\phi_t} \end{bmatrix}, \quad \mathbf{M} = \begin{bmatrix} M_{uu} & 0 & 0 \\ 0 & M_{\phi_y\phi_y} & 0 \\ 0 & 0 & M_{\phi_t\phi_t} \end{bmatrix} \quad (20)$$

Thus, the NURBS-based IGA flow chart is depicted in Fig. 4 to analyze the free vibration of a Timoshenko curved beam. Firstly, the exact NURBS geometric information is extracted from the curved beam model without subdivision. Next, the refinement of IGA is implemented according to the requirement of calculation, in which the geometric model remains unchanged. Then, the computer program runs directly on the refined NURBS geometries without any conversion of data format. Finally, the analysis results can be obtained by the corresponding control variables. In this study, the k -refinement is adopted to achieve C^{p-1} -continuity for NURBS of polynomial order p .

3. Numerical locking and effective scheme for free vibration of curved beams

Numerical locking may exist in slender Timoshenko beam solved by displacement-based finite element method, usually occurring in the case of low-order polynomial interpolation. Straight beam mainly involves shear locking, however for curved beam, additional locking is also included due to the influence of its curvature. Locking effect is attributed to the interpolation of inconsistent order for displacement components participating in strain terms in FEM (Ishaquddin *et al.* 2012). Currently, isogeometric analysis (Hughes *et al.* 2005) demonstrated its superiority in numerical precision, efficiency and integration of CAD and CAE. However, it is shown that the NURBS element suffers from numerical locking for static analysis, in which the locking effect leads the numerical solution of displacement to exhibit stiff behavior for low-order NURBS element under some parametric condition such as slender region (Echter and Bischoff 2010).

Among the several existing methods for overcoming locking effect, the selective reduced integration techniques have been studied and improved for decades of years due to the simplicity of implementation (Adam *et al.* 2014). In addition, a strain projection method (\bar{B} method) was applied in NURBS element to treat volumetric locking (Elguedj *et al.* 2008) and in-plane locking of static Timoshenko curved beam recently (Bouclier *et al.* 2012). Therefore, the two techniques are adopted jointly in this work to solve both in-plane and out-of-plane locking within the context

of free vibration analysis. Note that there are the same number of Gauss points in stiffness and mass matrices for the full and reduced integration herein. However, the selective reduced integration is only implemented in the stiffness matrices.

3.1 In-plane model: shear and membrane locking

For in-plane case, there is inconsistency of derivative order in both membrane and transverse shear strain components, namely the interpolation functions cannot represent the so-called inextensible bending and shearless bending ($\varepsilon=0$ and $\gamma=0$ in Eq. (7)) for thin beam model, resulting in the well-known membrane locking and shear locking. Thus in this section, various selective integral schemes in conjunction with the \bar{B} (also expressed as $Bbar$ thereafter) projection element are compared for free vibration of curved beam with a wide range of slenderness to achieve locking free analysis.

The detailed theoretical basis of \bar{B} projection method can be seen in the reference (Elguedj *et al.* 2008, Bouclier *et al.* 2012), in which the strains relating to locking (membrane and transverse shear strains) are projected to a basis of lower dimension. Namely, the modified \bar{B} projection stiffness matrices (Bouclier *et al.* 2012) can be written as

$$[K_{\bar{B}}] = [\bar{K}_m] + [\bar{K}_s] + [K_b] \quad (21)$$

where \bar{K}_m and \bar{K}_s are the stiffness matrixes related to the modified membrane and transverse shear strains, respectively, and K_b is the bending stiffness matrix.

Arbitrary slenderness: The 1/4 circular arch with hinged-hinged boundary conditions is examined here as shown in Fig. 5 with the main parameters as: radius $R=1$ m, arc length $L=R\theta$, radius of gyration $r = \sqrt{I/A}$, central angle $\theta=\pi/2$, $E=10$ GPa, $k=5/6$, Poisson ratio $\nu=0.3$. The dimensionless frequency parameter is defined as $\lambda_i = \omega_i L^2 \sqrt{\rho A / EI}$, ω_i denotes the i th natural frequency, and ρ is the material density. The isogeometric free vibration analysis is implemented from $p=2$ through k -refinement in this study due to the fact that quadratic NURBS is the lowest order that can represent exact curved beam model. Therefore, full integration (3-point for $p=2$ and 4-point for $p=3$), various selective reduced integral schemes and \bar{B} projection element are tested in this example for comparison, with different combination of numbers corresponding to Gauss integration point for bending, membrane and shear energy terms, respectively. For instance, 2-1-1 means that 2-point integration is adopted for bending energy terms and 1-point integration for membrane and transverse shear energy terms. It is important to note that there are almost the same results for 2-point, 3-point and 4-point integration for \bar{B} projection elements. Hence, several representative solutions for frequency parameters with better accuracy obtained by twenty quadratic and cubic NURBS elements along with the analytic solutions (Blevins 1979) are depicted in Fig. 6 for comparison.

Clearly, there are serious locking effects for 3-point integration in quadratic NURBS element in Fig. 6(a), because the fundamental frequency parameters deviate from the analytic solutions remarkably when the slenderness ratio (R/r) is larger than 1000, though the subdivision number of element is twenty. And the improvements exist in \bar{B} projection element and reduced 2-point integration, selective reduced integration (3-2-2) to some extent, but they are not optimal for extremely thin curved beams. Relatively, locking free analysis can be achieved only by selective reduced integration 2-1-1 and 3-1-1 for quadratic NURBS, that is 1-point integration adopted for

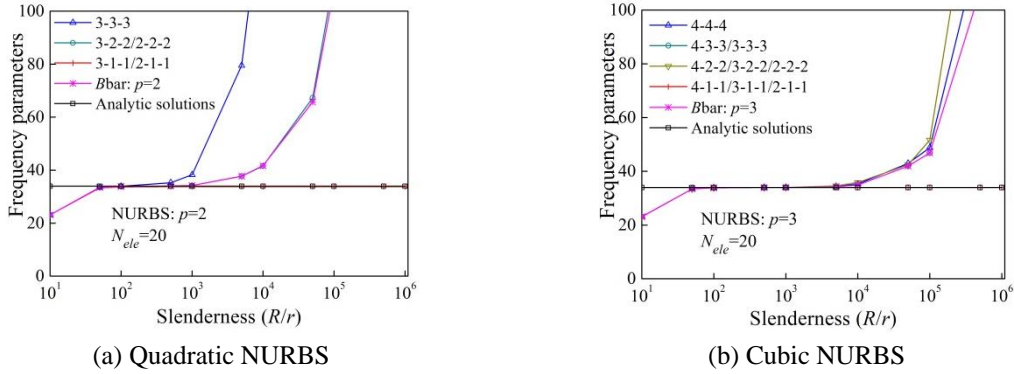


Fig. 6 Comparison for the fundamental frequency parameters of hinged-hinged 1/4 circular beam by selective reduced integration and NURBS \bar{B} element

both membrane and shear energy terms. Moreover, the locking regions are backward distinctly for cubic NURBS in Fig. 6(b), and only by 1-point integration there is no locking effect under the circumstance of extremely slender model. Herein, an additional Gauss point is incorporated to the boundary element for 1-point integration to remove the zero-energy mode (Bouclier *et al.* 2012, Adam *et al.* 2014).

Slenderness $R/r=100$: The curved beam with slenderness $R/r=100$ is studied with the exact solution (Tufekci and Arpacı 1998) for reference and the relative error of frequency parameter is defined as

$$|\lambda_i - \lambda_{iRef}| / \lambda_{iRef} \times 100\% \quad (22)$$

where i denotes the i th mode, λ_i is the numerical solution of frequency parameter and λ_{iRef} is the exact solution for reference.

Although there is no severe locking effect for the fundamental frequency of curved beam with slenderness $R/r=100$ in Fig. 7(a), the full integration (3-point) in quadratic NURBS elements is inappropriate for the fundamental frequency of moderately thin curved beam. Apart from \bar{B} projection elements, better results are achieved with 2-point integration, and the accuracy comparison of various integral selections is shown in Fig. 7(b). By contrast of Figs. 7(a) and (b), there are the equivalent effects for integration of 2-point (2-2-2) and 3-2-2 along with \bar{B} projection element, being optimal in the optional integral schemes.

Notably, the membrane-to-shear stiffness ratio $EA/GA=2.6$ is greater than 1, and thus the membrane energy term has the larger proportion. Accordingly, the curved beam in this case tends to be membrane locking relatively rather than shear locking, though both of the two numerical locking are not dominated. It can well explain that, there are better results for 1-point reduced integration in membrane energy term (namely 2-1-2 or 3-1-2) in Fig. 7(b) when the subdivision levels of elements are still fairly rough due to obvious locking effect in this region. However, this is not the case for 1-point integration in shear energy term (2-2-1). Further, for the cubic NURBS shown in Figs. 8(a) and (b), there is no significant difference for the 1st and 5th frequency with various integration schemes, and desired results are obtained with the fine element subdivision. Therefore, the cubic NURBS hardly suffers from numerical locking for the curved beam with $R/r=100$, which is also observed in Fig. 6(b) clearly.

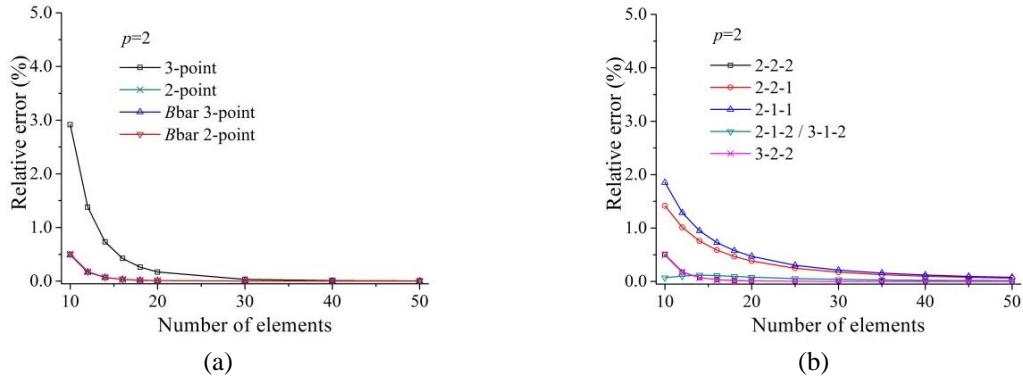


Fig. 7 Convergence comparison of fundamental frequency for curved beam with $R/r=100$ by quadratic NURBS with respect to various schemes

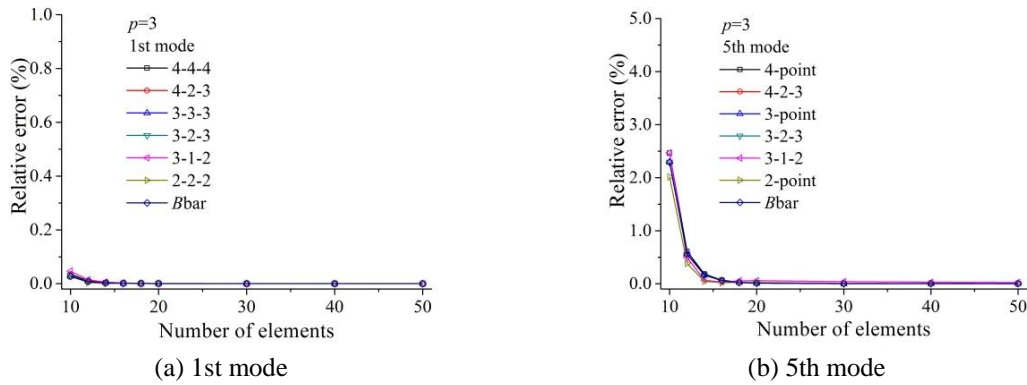


Fig. 8 Convergence comparison of the 1st and 5th frequency for curved beam with $R/r=100$ by cubic NURBS with respect to various schemes

Overall, the \bar{B} projection element, reduced 2-point (2-2-2) integration and selective reduced 3-2-2 integration (3-point for bending energy terms and 2-point for membrane and transverse shear energy terms) are feasible integral schemes in C^1 -continuous quadratic elements for free vibration analysis of curved beam with slenderness $R/r=100$.

3.2 Out-of-plane numerical locking

As shown in Eq. (18), for the out-of-plane free vibration of planar curved beam taking into account the effects of shear deformation and rotary inertia, all of the three strain terms have the coupling of derivatives with zero and the first order together for displacement components, resulting in the curvature related locking as discussed for the in-plane counterpart. However, differing from the in-plane pattern, it is difficult to determinate in advance for which energy term the reduced integration or \bar{B} projection method should be performed to eliminate numerical locking, because of the interpolation of inconsistent order existing in all the three strains. In view of the feature of out-of-plane locking, the integral scheme based on model parameters of curved beam presented below exhibits its effectiveness.

Herein, the curved beam with circular cross-section and clamped-clamped boundary conditions are considered with the radius of cross section r_{cs} , $\nu=0.3$ and shear modulus $G=E/2(1+\nu)$, namely $EI/GA=0.65r_{cs}^2$, $EI/GJ=1.3$. In this curved beam model, the bending-to-twisting stiffness ratio keeps constant also close to 1, while the bending-to-shear stiffness ratio changes with the value of radius r_{cs} , thus shear locking may be dominated. And let $r_{cs}=1$, the other main parameters are listed as: $k=0.89$, $A=\pi \text{ m}^2$, $I_y=\pi/4 \text{ m}^4$, $J=I_p=\pi/2 \text{ m}^4$, $E=2.6\times 10^{-2} \text{ GPa}$, and the dimensionless frequency parameters $\lambda = \omega R^2 \sqrt{\rho A / EI_y}$. Accordingly, the stiffness ratio $GJ : GA : EI_y = 1 : 2 : 1.3$, and the proportion of shear energy terms is the largest among the three terms. Therefore, by \bar{B} projection method, the shear strain is projected onto a basis of lower dimension, but the twisting and bending strains are not projected. Thus, it yields $[K_{\bar{B}}] = [K_t] + [\bar{K}_s] + [K_b]$.

Arbitrary slenderness: The dimensionless fundamental frequency parameters of 60° and 90° circular beam calculated by basic quadratic and cubic NURBS elements along with \bar{B} projection element are presented in Fig. 9 in contrast with the analytic solutions (Blevins 1979), in which full integration is adopted for observation of locking phenomenon. Obviously, the solutions by \bar{B} projection element are completely free from locking, while there are severe locking effects for basic quadratic and cubic NURBS elements in extremely slender cases. It is noted that, selective reduced 1-point integration does not work in this case which is locking free for the in-plane models, because of the complexity of out-of-plane locking.

Slenderness $R/r=100, 20$: The accuracy of natural frequencies may be affected by numerical locking especially for coarse meshes, though there is no serious influence according to the results in Fig. 9 for moderately thin curved beams. The convergence of fundamental frequencies is illustrated in Figs. 10(a) and (b) for curved beam with 60° opening angle and different integral schemes by using quadratic NURBS elements for $R/r=100$ and 20 , respectively. Moreover, the exact solution are from the references (Howson and Jemah 1999, Tufekci and Dogruer 2006) and the different combination of numbers correspond to Gauss integration for twisting, shear and bending energy terms, separately.

It is seen that the gap between the two ranges (0~12% and 0~0.5%) of relative error are fairly wide for $R/r=100$ and 20 , respectively. The slender beam corresponds to the lower accuracy of frequency parameters. From Fig. 10, the reduced 2-point integration or 2-point integration only in shear energy term exhibits better convergence than the other integral schemes, and only five of the

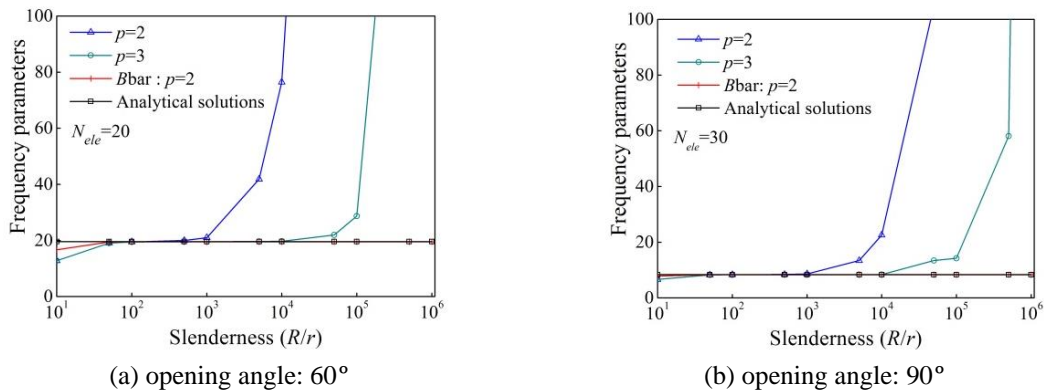


Fig. 9 Numerical locking effect of fundamental frequency for out-of-plane curved beam model

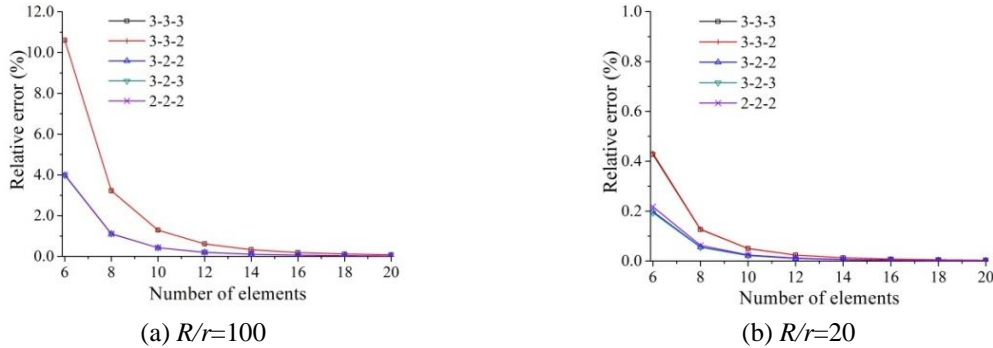


Fig. 10 Convergence comparison of fundamental frequency for out-of-plane curved beam model with different integral schemes by quadratic NURBS

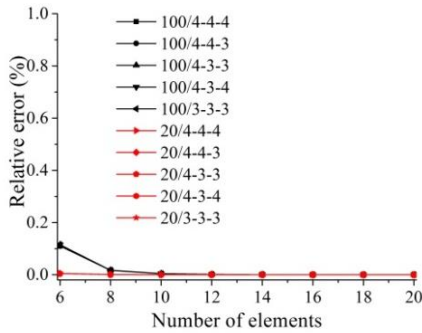


Fig. 11 Convergence comparison for cubic NURBS

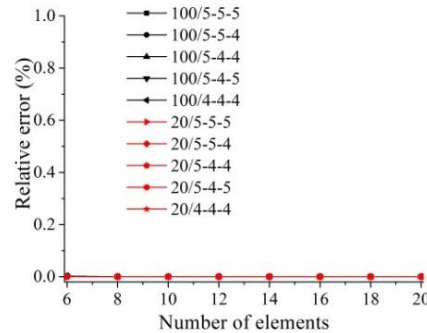


Fig. 12 Convergence comparison for quartic NURBS

relatively high accuracy are shown here. Then by using k -refinement, different integral selections of cubic NURBS for $R/r = 100$ and 20 are shown in Fig. 11. The accuracy is greatly enhanced and there is no significant difference for various integral selections no matter $R/r = 100$ or 20 . When the subdividing elements are less than ten, there are still small accuracy gaps for the two slenderness ratios, but both of them obtain accurate results with the fine subdivision. Next, the order of NURBS is elevated to quartic and the convergence comparison is shown in Fig. 12. Obviously, both of them acquire consistent convergence, and the frequency results are in excellent agreement with the exact solution. Note that there are only 10 control points in total for $N_{ele}=6$, while the finite element method requires 25 nodes, namely with relatively few degrees of freedom.

To sum up, there are locking effects for IGA-based free vibration of Timoshenko curved beam, in which C^1 -continuous quadratic and C^2 -continuous cubic NURBS elements suffer from numerical locking severely in extremely slender models for both in-plane and out-of-plane patterns. The selective reduced 1-point integration is free from membrane and shear locking of in-plane case. Nevertheless, it is not suitable for out-of-plane locking due to its special characteristic. Through numerical tests, the \bar{B} projection element based on stiffness ratio can achieve locking free analysis for out-of-plane vibration. Moreover, for moderately thin beam models ($R/r=100\sim 20$), full integration (3-point) is not the best option for quadratic NURBS, and reduced 2-point integration and selective reduced integration based on model parameters as well as \bar{B} projection element can obtain better results. Finally, the cubic and higher order NURBS exhibits

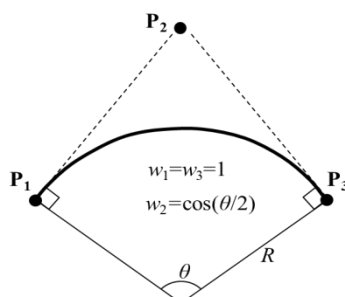


Fig. 13 Geometric configuration of circular beam by quadratic NURBS

negligible locking effect for moderately slender models, and also shows little difference for various integral schemes.

4. Numerical examples for in-plane and out-of-plane free vibration of curved beams

For the circular curved beam, the geometric configuration is shown in Fig. 13 by a quadratic NURBS curve. Actually, a single NURBS patch is adequate to construct the curved beam model with the opening angle less than 180° . The NURBS curve has the first and last control points P_1 and P_3 interpolatory, the associated weights $w_1, w_3=1$, and the internal control points (P_2) non-interpolatory, $w_2=\cos(\theta/2)$. When the opening angle is greater than 180° , the model can be constructed using a NURBS curve with several patches and C^0 -continuity at each boundary (Cottrell *et al.* 2009). Herein, a single patch is utilized to analyze the curved beam models, which can be easily extended to multi-patch case. In addition, the NURBS geometric information of non-circular curved beam such as parabolic and elliptical beams can be provided exactly from CAD model. The following numerical examples aim to illustrate the superiority of IGA method for in-plane and out-of-plane free vibration analysis of curved beams with usual slenderness $R/r \leq 100$, complex shape and variable curvature.

4.1 Uniform circular Timoshenko curved beam

Example 1: Accuracy and efficiency of IGA elements with C^{p-1} continuity

A quarter of circular beam is considered to analyze the in-plane free vibration using IGA with exact natural frequencies (Eisenberger and Efraim 2001) and FEM numerical solutions (Yang *et al.* 2008) presented for comparison. This example mainly discusses hinged-hinged and clamped-clamped boundary conditions. The related parameters about geometry and material are given as: $R/r=15$ (hinged-hinged), $R/r=15.9155$ (clamped-clamped), $r=\sqrt{I/A}$, $k=0.85$, $E=70$ GPa, and $kG/E=0.3$ (Yang *et al.* 2008).

Ten curved beam elements with cubic polynomial basis functions in FEM were employed in Yang *et al.* 2008, for each of which there are 4 nodes, totally 31 nodes. To compare with the FEM solutions, the initial curved beam model is subdivided into 10 and 28 cubic NURBS elements by k -refinement. Due to the C^2 continuity between elements, there are 13 and 31 control points for the two refinement levels, respectively. According to the locking investigation in Section 3.1, the

Table 1 Comparison of frequency parameters for the 1/4 circular beam with hinged-hinged and clamped-clamped boundary conditions

Mode number	Hinged-hinged				Clamped-clamped			
	$N_{ele}: 10$ $N_{cp}: 13$	$N_{ele}: 28$ $N_{cp}: 31$	Eisenberger and Efraim 2001	Yang <i>et al.</i> 2008	$N_{ele}: 10$ $N_{cp}: 13$	$N_{ele}: 28$ $N_{cp}: 31$	Eisenberger and Efraim 2001	Yang <i>et al.</i> 2008
1	29.2802	29.2799	29.2799	29.306	36.7033	36.7031	36.7031	36.657
2	33.3050	33.3049	33.3049	33.243	42.2644	42.2635	42.2635	42.289
3	67.1291	67.1235	67.1235	67.123	82.2454	82.2330	82.2330	82.228
4	79.9726	79.9708	79.9708	79.950	84.4941	84.4915	84.4915	84.471
5	107.9012	107.8512	107.8511	107.844	122.3905	122.3054	122.3053	122.298
6	143.7909	143.6177	143.6175	143.679	155.1085	154.9448	154.9447	154.998
7	156.8114	156.6657	156.6656	156.629	168.4921	168.2028	168.2026	168.174
8	191.8435	190.4778	190.4771	190.596	206.2256	204.4727	204.4718	204.599
9	225.5067	225.3612	225.3611	225.349	239.1456	238.9921	238.9920	238.973
10	239.6933	234.5258	234.5235	234.809	255.1369	249.0140	249.0114	249.320

effect of axis extensibility and shear deformation cannot be neglected for curved beam with $R/r \leq 20$, hence full integration ($p+1$ point) is adopted here.

The first 10 frequency parameters with hinged-hinged and clamped-clamped boundary conditions are listed in Table 1, in which N_{ele} and N_{cp} represent the number of NURBS elements and the corresponding control points respectively. Compared to the exact natural frequencies (Eisenberger and Efraim 2001), it is seen that the precision of the first 2 frequency parameters by IGA are higher than those by FEM (Yang *et al.* 2008) for the two boundary conditions when N_{ele} equals 10. However, it is not the same case for the relative higher-order frequency parameters. Note that there are only 13 control points in IGA compared with 31 nodes in FEM, namely the less number of degrees of freedom are used for IGA herein. Thus, through further subdivision to 28 elements and 31 control points, the frequency results of IGA are in excellent agreement with the exact solutions. In fact, due to the C^{p-1} continuity of NURBS elements obtained by k -refinement, there are local sharing properties for the NURBS control points. Therefore, the IGA solutions present higher accuracy than the FEM solutions with the identical number of degrees of freedom.

Meanwhile, the first 9 modal shapes of hinged-hinged boundary conditions obtained by 28 cubic NURBS elements are demonstrated in Figs. 14(a)-(i), and the almost consistent modal shapes can be found in the references (Eisenberger and Efraim 2001, Yang *et al.* 2008).

Example 2: In-plane free vibration of uniform circular arches

The uniform circular arches with hinged-hinged and clamped-clamped boundary conditions and slenderness $R/r=50, 75$ and 100 are considered. The first 5 dimensionless natural frequencies of arches are shown in Tables 2 and 3 by cubic NURBS with the opening angle of $90^\circ, 120^\circ$ and 150° . Based on the comparison of integration schemes in Fig. 8, almost consistent convergence can be obtained, thus fifty elements with 3-point integration are employed here. It can be observed from Tables 2 and 3 that, the IGA results agree well with the exact solutions in Tufekci and Arpacı (1998), and the natural frequencies of arch may be affected by constraint conditions and opening angles. Specifically, the arch structures with clamped-clamped ends have greater stiffness than the hinged ones, leading to the higher natural frequencies. To further describe the influence of opening

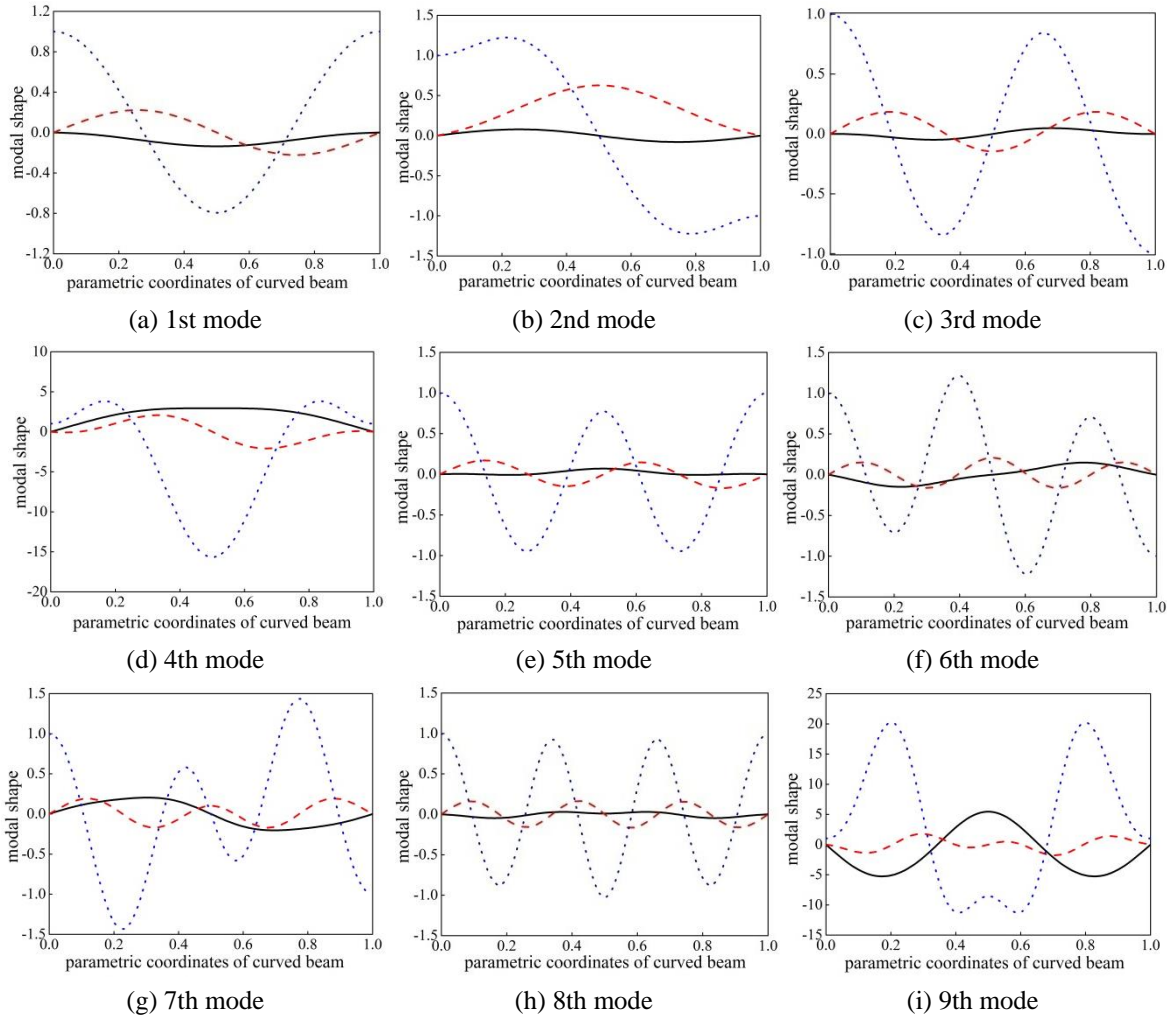


Fig. 14 The first 9 modal shapes of 1/4 circular beam with hinged-hinged boundary condition (The black, red/dash and blue/dot curves represent u , w and θ , respectively)

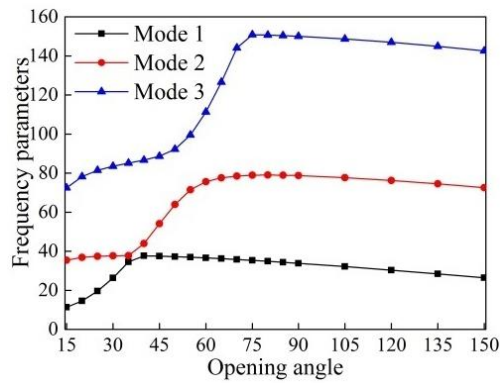


Fig. 15 Influence of opening angle on natural frequency of arch with hinged-hinged end

Table 2 Frequency parameters $\lambda = \omega R^2 \theta^2 \sqrt{\rho A / EI}$ for uniform hinged-hinged arch

R/r	Mode	90°		120°		150°	
		Tufekci and Arpaci 1998	IGA	Tufekci and Arpaci 1998	IGA	Tufekci and Arpaci 1998	IGA
100	1	33.8341	33.8341	30.3178	30.3178	26.4079	26.4079
	2	78.7259	78.7261	76.2373	76.2375	72.5587	72.5588
	3	150.0300	150.0312	146.9290	146.9298	142.5925	142.5933
	4	214.8133	214.8138	229.9762	229.9740	227.9351	227.9357
	5	259.7674	259.7633	339.1900	339.1539	336.4950	336.4769
75	1	33.7367	33.7368	30.2665	30.2665	26.3787	26.3787
	2	77.7025	77.7029	75.8395	75.8397	72.3473	72.3474
	3	148.4183	148.4198	145.9973	145.9987	141.9974	141.9981
	4	173.9414	173.9468	225.3067	225.3078	226.0291	226.0300
	5	239.3448	239.3443	321.9759	321.9895	333.3854	333.3658
50	1	33.4632	33.4635	30.1212	30.1214	26.2958	26.2958
	2	74.3412	74.3435	74.6949	74.6957	71.7477	71.7483
	3	121.4958	121.5088	143.4124	143.4163	140.3306	140.3326
	4	144.0231	144.0274	197.2652	197.2830	219.9901	219.9955
	5	226.3381	226.3464	242.4045	242.4112	324.5391	324.5281

Table 3 Frequency parameters $\lambda = \omega R^2 \theta^2 \sqrt{\rho A / EI}$ for uniform clamped-clamped arch

R/r	Mode	90°		120°		150°	
		Tufekci and Arpaci 1998	IGA	Tufekci and Arpaci 1998	IGA	Tufekci and Arpaci 1998	IGA
100	1	55.3434	55.3436	51.7045	51.7046	47.5326	47.5326
	2	102.3868	102.3876	101.9366	101.9372	98.8691	98.8697
	3	188.4994	188.5014	185.7236	185.7249	181.2108	181.2116
	4	219.1514	219.1515	269.2141	269.2139	271.5375	271.5351
	5	299.1958	299.1832	393.7767	393.7655	391.9823	391.9661
75	1	55.9768	54.9771	51.5012	51.5014	47.4091	47.4092
	2	98.5094	98.5111	100.6416	100.6427	98.2165	98.2172
	3	174.9116	174.9162	183.7216	183.7238	179.9086	179.9100
	4	185.1081	185.1109	253.5605	253.5653	266.9185	266.9221
	5	284.7500	284.7454	332.4988	332.5134	386.3414	386.3178
50	1	53.9660	53.9670	50.9322	50.9328	47.0612	47.0616
	2	86.1908	86.1971	96.8517	96.8548	96.3684	96.3702
	3	132.7272	132.7371	178.1998	178.2046	176.2864	176.2897
	4	175.8392	175.8474	198.0489	198.0698	250.0629	250.0759
	5	265.8141	265.8241	282.9555	282.9695	338.9705	338.9982

angles, the first three frequency parameters of arches with opening angles from $15^\circ \sim 150^\circ$ are demonstrated in Fig. 15 with taking hinged-hinged boundary condition as an example. It is seen that there is no consistent monotonicity for the three curves, due to the conversion of vibration modes of arch.

Example 3: Out-of-plane free vibration of uniform circular arches

The circular curved beams with constant circular cross-section and clamped-clamped boundary condition are considered firstly, and their main parameters (Howson and Jemah 1999, Ye and Zhao 2012) are listed as: $\nu=0.3$, $k=0.89$, $A=\pi \text{ m}^2$, $I_y=\pi/4 \text{ m}^4$, $J=I_p=\pi/2 \text{ m}^4$, $R=20\sqrt{I_y/A}$. Table 4 presents the values of the first four dimensionless natural frequencies $\lambda_i = \omega_i R^2 \sqrt{\rho A / EI_y}$ for 60° and 120° circular arches with k -refinement scheme. According to the comparison of various integral schemes in Figs. 10-12, the 3-2-2 integration is adopted for $p=2$ and full integration is utilized for $p=3$ and 4.

The calculated results in Table 4 are refined from 5~50 elements, and compared with the exact solutions (Howson and Jemah 1999, Tufekci and Dogruer 2006, Ye and Zhao 2012). The accuracy for quadratic NURBS elements is gradually increased with the element subdivision. For cubic or quartic NURBS, the precise results can be achieved even for the coarse refinement levels. Moreover, the frequency solutions obtained by 30 cubic elements and 20 quartic elements are in

Table 4 First 4 dimensionless natural frequencies for 60° and 120° circular curved beams with k -refinement schemes

Order	N_{ele}	Mode (opening angle 60°)				Mode (opening angle 120°)			
		1	2	3	4	1	2	3	4
$p=2$	5	16.96142	39.70332	41.85272	75.76912	4.467895	12.95843	23.27310	29.10392
	10	16.88865	39.70053	40.96557	70.76255	4.31657	11.83191	22.67829	23.31065
	20	16.88516	39.70037	40.93568	70.58891	4.309827	11.79763	22.51649	23.30297
	30	16.88499	39.70036	40.93438	70.58207	4.309495	11.79628	22.51132	23.30277
	50	16.88495	39.70036	40.93411	70.58071	4.309425	11.79600	22.51035	23.30274
$p=3$	5	16.88762	39.70041	41.03895	71.84812	4.315583	11.97866	23.25486	24.29330
	10	16.88497	39.70036	40.93479	70.58822	4.309467	11.79713	22.52211	23.30318
	20	16.88495	39.70036	40.93408	70.58058	4.309415	11.79598	22.51031	23.30274
	30	16.88495	39.70036	40.93407	70.58052	4.309415	11.79597	22.51022	23.30273
	50	16.88495	39.70036	40.93407	70.58051	4.309414	11.79597	22.51022	23.30273
$p=4$	5	16.88504	39.70036	40.94408	70.81863	4.309943	11.82554	22.88458	23.32965
	10	16.88495	39.70036	40.93409	70.58081	4.309415	11.79600	22.51094	23.30276
	20	16.88495	39.70036	40.93407	70.58051	4.309414	11.79597	22.51022	23.30273
	30	16.88495	39.70036	40.93407	70.58051	4.309414	11.79597	22.51022	23.30273
	50	16.88495	39.70036	40.93407	70.58051	4.309414	11.79597	22.51022	23.30273
Tufekci and Dogruer 2006		16.88495	39.70036	40.93407	70.58051	4.309414	11.79597	22.51022	23.30273
Howson and Jemah 1999		16.885	39.700	40.934	70.581	4.3094	11.796	22.510	23.303
Ye and Zhao 2012		16.885	39.700	40.934	70.581	4.3094	11.796	22.510	23.303

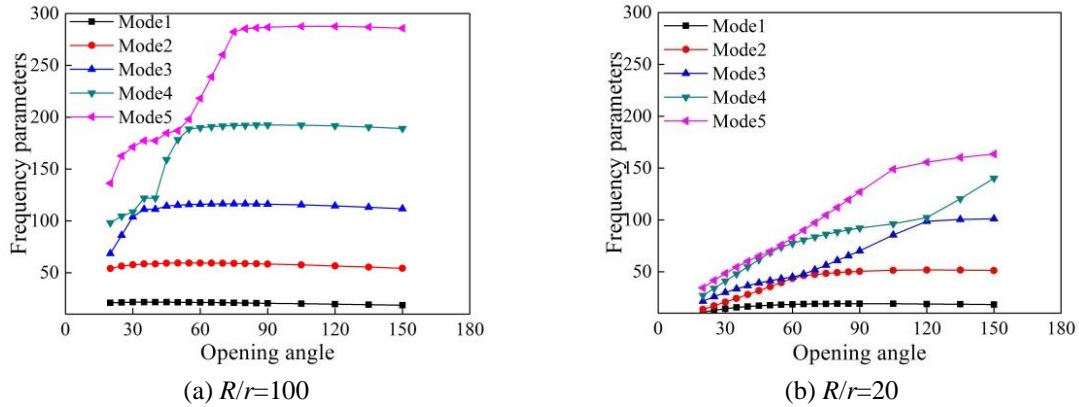


Fig. 16 Relation between opening angle and natural frequency with clamped-clamped end

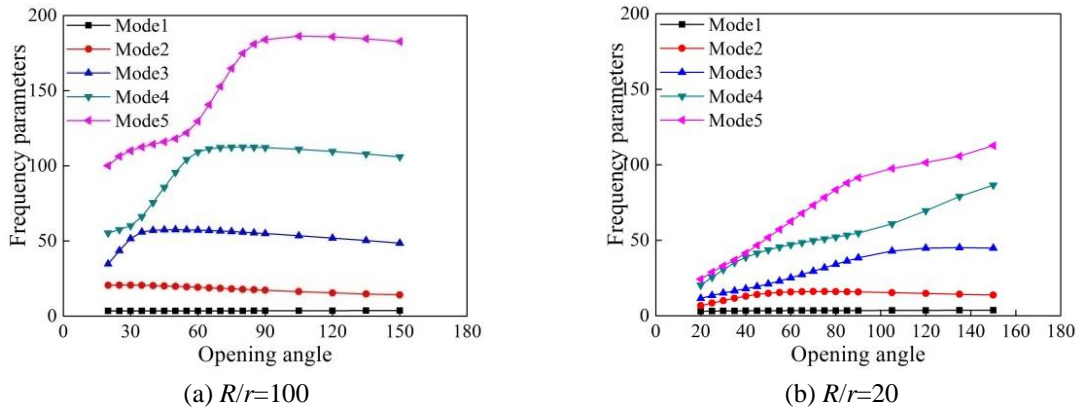


Fig. 17 Relation between opening angle and natural frequency with clamped-free end

excellent agreement with those in the references (Howson and Jemah 1999, Tufekci and Dogruer 2006, Ye and Zhao 2012).

To further study the influence of opening angle on the natural frequencies of circular arches, the values related to various opening angles are calculated by 20 quartic NURBS elements. The obvious change of monotonicity mainly exist in the range of 20°~150°, hence the relation of the first five natural frequencies with clamped-clamped and clamped-free ends are shown in Figs. 16 and 17 for $R/r=100$ and 20, respectively. To sum up, the natural frequencies of arch with various opening angles yield large change, which is especially obvious for the higher order modes owing to the conversion of vibration mode. In addition, the relatively greater frequencies are acquired for slenderness $R/r=100$ than those for $R/r=20$, and the frequencies of curved beam with clamped-clamped end are greater than the corresponding frequencies with clamped-free end because of the stiffer constraints of the former.

4.2 Variable cross-section Timoshenko parabolic curved beam

Example 4: Parabolic curved beam with constant and variable cross-sections

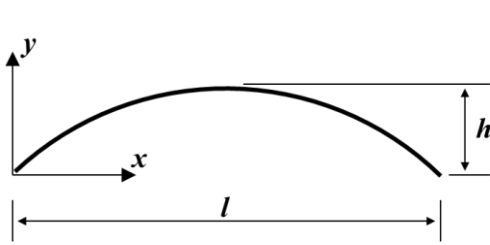


Fig. 18 Centroidal axis of parabolic curved beam

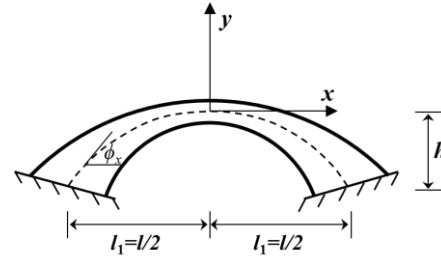


Fig. 19 Parabolic curved beam with varying cross section

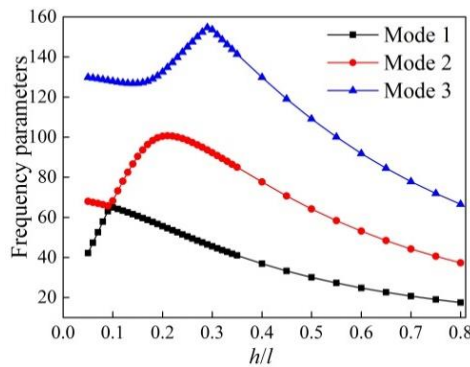


Fig. 20 Relation between h/l and natural frequency parameters with clamped-clamped end ($S=100$)

The NURBS employed in isogeometric analysis is powerful enough to describe the exact geometry of curved beam with variable curvature, and the computation process of IGA is convenient so that there is no additional effort needed in the specific geometric model of curved beam like in FEM. In this section, the parabolic geometry is considered to analyze the free vibration of both in-plane and out-of-plane curved beam models.

In-plane vibration: Free vibration of the parabolic beam in Figs. 18 and 19 with variable cross section is discussed, and the non-dimensional equation of parabolic beam (Oh *et al.* 1999, Huang *et al.* 1998) are given by

$$\eta = 4 f \zeta (1 - \zeta), \quad 0 \leq \zeta \leq 1 \tag{23}$$

$$I(x) = \frac{I_c}{[1 - (1 - \alpha)(|x|/l_1)] \cos \phi_x} \tag{24}$$

where, l is the span length of the parabolic beam and l_1 is half of the span length, $\eta = y/l$, $\zeta = x/l$; I_c is the moment of inertia at the middle of beam; A_c is the associated area of cross section; ϕ_x is the angle between the tangent and the horizontal axis; $\alpha=0.25, 0.5, 0.75$ and 1.0 ; $S = l / \sqrt{(I_c / A_c)}$ denotes the slenderness.

The first 6 dimensionless natural frequencies $\lambda_i = \omega_i l^2 \sqrt{\rho A / EI}$ together with the reference solutions (Huang *et al.* 1998) for clamped-clamped support are listed in Table 5 ($S=100, h/l=0.1$) and Table 6 ($S=50, h/l=0.4$). Based on the comparison of integration schemes in Fig. 7 in Section

Table 5 Dimensionless frequencies of in-plane free vibration of a parabolic beam with variable cross-sections ($S = 100, h/l=0.1$)

Mode	$\alpha=0.25$		$\alpha=0.5$		$\alpha=0.75$		$\alpha=1.0$	
	Huang <i>et al.</i> 1998	IGA						
1	70.8520	70.8506	64.9926	64.9742	60.2053	60.1914	56.7777	56.7671
2	72.9642	72.9385	68.2589	68.2578	66.5432	66.5425	65.2425	65.2423
3	139.8112	139.7733	127.9823	127.9608	120.8314	120.8214	115.7458	115.7447
4	217.8530	217.8716	200.6139	200.6635	189.4152	189.4919	181.0018	181.1023
5	316.0446	316.4323	293.7004	294.1300	278.7741	279.2537	267.3887	267.9175
6	340.8951	340.9163	327.5784	327.6066	319.0914	319.1305	312.9289	312.9830

Table 6 Dimensionless frequencies of in-plane free vibration of a parabolic beam with variable cross-sections ($S = 50, h/l=0.4$)

Mode	$\alpha=0.25$		$\alpha=0.5$		$\alpha=0.75$		$\alpha=1.0$	
	Huang <i>et al.</i> 1998	IGA						
1	39.5830	39.5339	34.9439	34.9094	32.2111	32.1844	30.2780	30.2565
2	78.3612	78.2272	71.5691	71.4733	67.3029	67.2299	64.1796	64.1227
3	90.6192	90.6142	87.7266	87.7238	85.9828	85.9809	84.7632	84.7621
4	124.6073	124.3688	115.8481	115.6878	109.9981	109.8887	105.5253	105.4536
5	145.2034	145.1974	139.3936	139.3918	135.9329	135.9331	133.5337	133.5353
6	176.9525	176.6746	166.4010	166.2672	159.0894	159.0542	153.3831	153.4235

3.1, twenty quadratic NURBS elements are adopted by 2-point integration here, and the calculated frequencies are in close agreement with the reference solutions. Moreover, it can be observed from Fig. 20 that the ratio of high to span length h/l affects clearly the first three frequencies.

Out-of-plane vibration: The parabolic beam with constant cross section in Fig. 18 is considered here, with the equation (Ye and Zhao 2012)

$$y = 0.8x - 0.02771x^2 \tag{25}$$

The main parameters are taken as: $E=26$ GPa, $E/G=2.6$, $k=0.833$, $L=28.87$ m, $h=5.774$ m, $A=3$ m², $I_y=0.25$ m⁴, $I_p=2.5$ m⁴, $J=0.79$ m⁴, and $\rho=2166.67$ kg/m³. Based on the comparison of Fig. 10 in Section 3.2, the 2-point integration is adopted here to eliminate numerical locking. Accordingly, for clamped-clamped, clamped-hinged and hinged-hinged supports, the first 6 dimensionless natural frequencies $\lambda_i = \omega_i l^2 \sqrt{\rho A / EI}$ are listed in Table 7 together with the numerical solutions (Ye and Zhao 2012, Lee *et al.* 2008) for comparison. The frequencies acquired by 50 quadratic NURBS elements are almost identical with those by dynamic stiffness method (Ye and Zhao 2012). However, the element subdivision and order elevation are implemented automatically in IGA based on exact geometric model, and also by k -refinement, the high-order continuous elements can enhance the accuracy of free vibration analysis of parabolic beam.

Table 7 Dimensionless natural frequencies of out-of-plane free vibration of parabolic beam

Supports		Mode 1	Mode 2	Mode 3	Mode 4	Mode 5	Mode 6
Clamped -clamped	Lee <i>et al.</i> 2008	17.12	48.77	96.06	109.9	158.7	203.8
	Ye and Zhao 2012	17.044	48.399	95.023	109.93	156.50	203.77
	IGA	17.043	48.399	95.023	109.93	156.50	203.77
Clamped -hinged	Lee <i>et al.</i> 2008	11.15	39.10	82.61	109.8	141.4	203.8
	Ye and Zhao 2012	11.128	38.963	82.191	109.82	140.46	203.77
	IGA	11.128	38.963	82.191	109.82	140.46	203.77
Hinged -hinged	Lee <i>et al.</i> 2008	6.090	30.40	70.03	109.8	125.0	194.0
	Ye and Zhao 2012	6.0826	30.402	70.032	109.80	125.04	193.96
	IGA	6.0825	30.402	70.032	109.80	125.05	193.97

5. Conclusions

The free vibration analysis of Timoshenko curved beam is addressed by NURBS-based IGA considering in-plane and especially the out-of-plane patterns in this paper. Actually, the C^{p-1} -continuous NURBS elements present obviously higher accuracy than the finite elements with the same degrees of freedom. However, their convergence and accuracy are also affected by numerical locking for both of the two patterns, especially when $p=2$, which is the lowest order of NURBS that can represent exact curved beam model. For extremely slender models, there is severely locking effect for quadratic and cubic elements by full integration. It involves membrane locking and shear locking for the in-plane pattern, while the other locking may exist in out-of-plane case due to interpolation of inconsistent order in all the three strains. Therefore, the selective reduced integration in conjunction with \bar{B} projection method are proposed to achieve locking free analysis for curved beam regardless of the extent of slenderness, and the accurate numerical results are also obtained in the non-dominated regions of locking effect.

Specifically, for extremely slender beams, the selective reduced one-point integration is free from membrane and shear locking of in-plane case, while \bar{B} projection element based on stiffness ratio can achieve locking free analysis for out-of-plane case. For curved beams with slenderness ratios $R/r=100\sim 20$ and both in-plane and out-of plane models, the reduced 2-point integration and selective reduced integration based on model parameters as well as \bar{B} projection element are good candidates for quadratic NURBS, and their locking effects are negligible for cubic or higher order NURBS.

In addition, the IGA computational model is directly utilized to the modal analysis of planar curved beams with variable curvature and complicated cross section, based on exact geometry, convenient implementation of k -refinement, and CAD and CAE integration. Moreover, the locking free schemes for vibration analysis of curved beam are applicable for distinct slenderness models. Finally, the influence factors of parameters of curved beams on their natural frequency are scrutinized, which facilitates the dynamic design of curved beams.

Acknowledgments

The supports of the National Natural Science Foundation of China (Grant Nos. 51478086 and

11332004), and the Key Laboratory Foundation of Science and Technology Innovation in Shaanxi Province (No. 2013SZS02-K02) are much appreciated.

References

- Adam, C., Bouabdallah, S., Zarroug, M. and Maitournam, H. (2014), "Improved numerical integration for locking treatment in isogeometric structural elements, Part I: Beams", *Comput. Meth. Appl. Mech. Eng.*, **279**, 1-28.
- Auciello, N.M. and Rosa, M.A. (1994), "Free vibrations of circular arches: a review", *J. Sound Vib.*, **176**(4), 433-458.
- Ball, R.E. (1967), "Dynamic analysis of rings by finite differences", *ASCE J. Eng. Mech. Div.*, **93**, 1-10.
- Bickford, W.B. and Strom, B.T. (1975), "Vibration of plane curved beams", *J. Sound Vib.*, **39**, 135-146.
- Blevins, R.D. (1979), *Formulas for Natural Frequency and Mode Shape*, Van Nostrand Reinhold Company, New York, USA.
- Bouclier, R., Elguedj, T. and Combescure, A. (2012), "Locking free isogeometric formulations of curved thick beams", *Comput. Meth. Appl. Mech. Eng.*, **245-246**, 144-162.
- Chidamparam, P. and Leissa, A.W. (1993), "Vibrations of planar curved beams, rings, and arches", *ASME Appl. Mech. Rev.*, **46**(9), 476-483.
- Cottrell, J.A., Hughes, T.J.R. and Bazilevs, Y. (2009), *Isogeometric Analysis: Toward Integration of CAD and FEA*, John Wiley & Sons Ltd., London, UK.
- Cottrell, J.A., Reali, A., Bazilevs, Y. and Hughes, T.J.R. (2006), "Isogeometric analysis of structural vibrations", *Comput. Meth. Appl. Mech. Eng.*, **195**(41-43), 5257-5296.
- Echter, R. and Bischoff, M. (2010), "Numerical efficiency, locking and unlocking of NURBS finite elements", *Comput. Meth. Appl. Mech. Eng.*, **199**(5-8), 374-382.
- Eisenberger, M. and Efraim, E. (2001), "In-plane vibrations of shear deformable curved beams", *Int. J. Numer. Meth. Eng.*, **52**, 1221-1234.
- Elguedj, T., Bazilevs, Y., Calo, V.M. and Hughes, T.J.R. (2008), " \bar{B} and \bar{F} projection methods for nearly incompressible linear and non-linear elasticity and plasticity using higher-order NURBS elements", *Comput. Meth. Appl. Mech. Eng.*, **197**, 2732-2762.
- Howson, W.P. and Jemah, A.K. (1999), "Exact out-of-plane natural frequencies of curved Timoshenko beams", *ASCE J. Eng. Mech.*, **125**(1), 19-25.
- Huang, C.S., Tseng, Y.P., Chang, S.H. and Hung, C.L. (2000), "Out-of-plane dynamic analysis of beams with arbitrarily varying curvature and cross-section by dynamic stiffness matrix method", *Int. J. Solid. Struct.*, **37**(3), 495-513.
- Huang, C.S., Tseng, Y.P., Leissa, A.W. and Nieh, K.Y. (1998), "An exact solution for in-plane vibrations of an arch having variable curvature and cross section", *Int. J. Mech. Sci.*, **40**(11), 1159-1173.
- Hughes, T.J.R., Cottrell, J.A. and Bazilevs, Y. (2005), "Isogeometric Analysis: CAD, finite elements, NURBS, exact geometry and mesh refinement", *Comput. Meth. Appl. Mech. Eng.*, **194**, 4135-4195.
- Ishaquddin, M.D., Raveendranath, P. and Reddy, J.N. (2012), "Flexure and torsion locking phenomena in out-of-plane deformation of Timoshenko curved beam element", *Finite Elem. Anal. Des.*, **51**, 22-30.
- Ishaquddin, M.D., Raveendranath, P. and Reddy, J.N. (2013), "Coupled polynomial field approach for elimination of flexure and torsion locking phenomena in the Timoshenko and Euler-Bernoulli curved beam elements", *Finite Elem. Anal. Des.*, **65**, 17-31.
- Kang, B., Riedel, C.H. and Tan, C.A. (2003), "Free vibration analysis of planar curved beams by wave propagation", *J. Sound Vib.*, **260**(1), 19-44.
- Kang, K., Bert, C. and Striz, H. (1995), "Vibration analysis of shear deformation circular arches by the differential quadrature method", *J. Sound Vib.*, **181**(2), 353-360.
- Kim, B.Y., Kim, C.B., Song, S.G. and Beom, H.G. and Cho C.D. (2009), "A finite thin circular beam element for out-of-plane vibration analysis of curved beams", *J. Mech. Sci. Tech.*, **23**(5), 1396-1405.

- Kim, H.J., Seo, Y.D. and Youn, S.K. (2009), "Isogeometric analysis for trimmed CAD surfaces", *Comput. Meth. Appl. Mech. Eng.*, **198**(37-40), 2982-2995.
- Lee, B.K., Oh, S.J., Mo, J.M. and Lee, T.E. (2008), "Out-of-plane free vibrations of curved beams with variable curvature", *J. Sound Vib.*, **318**(1/2), 227-246.
- Lee, J. and Schultz, W.W. (2004), "Eigenvalue analysis of Timoshenko beams and axisymmetric Mindlin plates by the pseudospectral method", *J. Sound Vib.*, **269**, 609-621.
- Lee, S.J. and Park, K.S. (2013), "Vibrations of Timoshenko beams with isogeometric approach", *Appl. Math. Model.*, **37**(22), 9174-9190.
- Luu, A.T., Kim, N.I. and Lee, J. (2015), "Isogeometric vibration analysis of free-form Timoshenko curved beams", *Meccanica*, **50**(1), 169-187.
- Mochida, Y. and Ilanko, S. (2016), "Condensation of independent variables in free vibration analysis of curved beams", *Adv. Aircraft Spacecraft Sci.*, **3**(1), 45-59.
- Oh, S.J., Lee, B.K. and Lee, I.W. (1999), "Natural frequencies of non-circular arches with rotatory inertia and shear deformation", *J. Sound Vib.*, **219**(1), 23-33.
- Piegl, L. and Tiller, W. (1997), *The NURBS Book*, 2nd Edition, Springer-Verlag, New York, USA.
- Raveendranath, P., Gajbir, S.G. and Venkateswara, R. (2001), "A three-noded shear-flexible curved beam element based on coupled displacement field interpolations", *Int. J. Numer. Meth. Eng.*, **51**, 85-101.
- Tufekci, E. and Arpacı, A. (1998), "Exact solution of in-plane vibrations of circular arches with account taken of axial extension, transverse shear and rotatory inertia effects", *J. Sound Vib.*, **209**(5), 845-856.
- Tufekci, E., Dogruer, O.Y. (2006), "Out-of-plane free vibration of a circular arch with uniform cross-section: Exact solution", *J. Sound Vib.*, **291**, 525-538.
- Wang, D.D. and Zhang, H.J. (2014), "A consistently coupled isogeometric-meshfree method", *Comput. Meth. Appl. Mech. Eng.*, **268**, 843-870.
- Wang, D.D., Liu, W. and Zhang, H.J. (2013), "Novel higher order mass matrices for isogeometric structural vibration analysis", *Comput. Meth. Appl. Mech. Eng.*, **260**, 92-108.
- Wang, D.D., Liu, W. and Zhang, H.J. (2015), "Superconvergent isogeometric free vibration analysis of Euler-Bernoulli beams and Kirchhoff plates with new higher order mass matrices", *Comput. Meth. Appl. Mech. Eng.*, **286**, 230-267.
- Weeger, O., Wever, U. and Simeon B. (2013), "Isogeometric analysis of nonlinear Euler-Bernoulli beam vibrations", *Nonlin. Dyn.*, **72**(4), 813-835.
- Wu, J.S. and Chiang, L.K. (2003), "Free vibration analysis of arches using curved beam elements", *Int. J. Numer. Meth. Eng.*, **58**, 1907-1936.
- Yang, F., Sedaghati, R. and Esmailzadeh, E. (2008), "Free in-plane vibration of general curved beams using finite element method", *J. Sound Vib.*, **318**(4-5), 850-867.
- Ye, K.S. and Zhao, X.J. (2012), "Dynamic stiffness method for out-of-plane free vibration analysis of planar curved beams", *Eng. Mech.*, **29**(3), 1-8.